REVIEW

Colorful "Stars" in the Dark

Chao Jing [a], Yi-Tao Long [b,c,*]

[a] Shanghai Institute of Applied Physics, Chinese Academy of Sciences, Shanghai, 201800, PR China
[b] State Key Laboratory of Analytical Chemistry for Life Science; School of Chemistry and Chemical Engineering, Nanjing University, Nanjing, 210023, PR China
[c] Molecular Sensing and Imaging Center, Nanjing University, Nanjing, 210023, PR China

Abstract

Plasmonic nanoparticles such as Au and Ag with localized surface plasmon resonance (LSPR) property exhibit unique scattering and absorption features. The plasmonic scattering and absorption bands are mainly located at visible light region which can be easily applied in visual detections. By modulating the size, shape and composition of gold and silver colloid solutions, plenty of colorimetric methods have been designed for the detection of metal ions, biomolecules and environmental contaminants. For many years, the LSPR-based measurements are implemented in reagent tubes. Since 2000, the plasmon resonance scattering (PRS) light of metal nanoparticles captured by dark-field microscopy enables the investigation at the nanoscale dimension. Mono-dispersed nanoparticles under a dark-field microscope showed distinct scattering light spots, like colorful stars in the dark sky. The PRS light of a single nanoparticle opens a new way for ultra-sensitive sensing which eliminates the average effects in bulk and provides more accurate reaction information. Thus, individual nanoparticles with specific scattering colors are excellent nanoprobes in the applications of biology, physics, and chemistry. In this review, the plasmonics based colorimetric nanosensors are presented. Particularly, the application of *in-situ* PRS in the dynamically monitoring of electrocatalytic reactions is highlighted. We firstly introduce a short history of the discovery and development of plasmonic nanoparticles from the ancient artwork to the modern characterization techniques. Some factors including morphology, and dielectric constants that are correlated to the LSPR bands and scattering light colors are listed. Secondly, we demonstrate the use of single plasmonic nanoparticles as visualized color-coded nanoprobes. As the morphology of particles has strong effect on the PRS light, elegant sensors have been conceived by the etching and growth of nanoparticles with different sizes and shapes. On the other hand, the real-time monitoring of particle structure evolution could also reveal the mechanism of the material fabrication at the nanoscale. In addition, core-satellite nanostructures with various linkers are proposed as ultra-sensitive sensors according to the inter-particle coupling effect. Subsequently, we summarize several advanced techniques for nanoscale signal extraction and amplifications. For instance, to expand the application of colorimetric nanosensors, converting the colors into RGB values could clearly distinguish the subtle color changes. Combining with high-throughput signal processing method, thousands of nanoparticles can be rapidly analyzed, which can greatly enhance the measurement efficiency. Except the PRS color, the PRS intensity could also provide abundant information and is easier to be captured. A facile method by converting the PRS intensity of single nanoparticles into visible colors is presented, which is mighty suitable for the *in-situ* monitoring of fast electrochemical process with high time resolution.

Keywords: Plasmon resonance scattering; Dark-field microscopy; Color-coded sensor; Nanoscale electrochemistry; Single-nanoparticle detection

1. Introduction

When you watch the sky at night, have you thought about what if the stars have colors? It would be such a fantastic scene, but everyone knows that it is impossible. However, if we move the view from the extensive universal to the micro world, everything will become possible. Coinage metal nanoparticles such as Au, Ag, and Cu have unique LSPR feature which will generate strong

Received 14 December 2022; Received in revised form 9 February 2023; Accepted 20 February 2023
Available online 27 February 2023

* Corresponding author, Yi-Tao Long, Tel: (86)13761159439, E-mail address: yitaolong@nju.edu.cn.

https://doi.org/10.13208/j.electrochem.2218006

scattering light under incident light excitation [1−3]. Employing dark-field microscopy (DFM), the plasmon resonance scattering (PRS) spots of mono-dispersed plasmonic nanoparticles with specific colors will be captured, just like the colorful stars shining in the dark background [4,5]. DFM achieves the observation of a single particle at nanoscale dimension which overcomes the optical diffraction limitations. Taking advantages of the PRS spectroscopy of nanoparticles including high spatial resolution, high intensity, non-blinking and bleaching, plentiful label-free and non-invasive sensors have been developed [6−9]. Notably, combining DFM with electrochemistry, the nanoscale electrochemical reactions could be *in-situ* characterized [10−12].

Recently, several reviews have presented the fundamentals and applications of PRS of single nanoparticles [13−16]. However, most of the reviews focused on the scattering spectral wavelength and intensity dependent outputs. It is important to note that the visual color-coded measurements are also promising methods for sensing, such as *in-situ* fast and on-site detections [17−19]. For instance, gold and silver nanoparticles have been widely applied in the fields of environments, life science and food safety including the colorimetric detections of metal ions, biomolecules, pesticide residues and banned additives [20−22]. Therefore, in this minireview, we highlight the direct colorimetric sensing of single plasmonic nanoparticles based on DFM, especially in the fields of electrochemical and electrocatalysis. Remarkable nanoprobes, constructed by modulating the morphology and composition of particles, and inter-particle coupling, are demonstrated. Some advanced signal amplification and conversion methods for improving detection efficiency are discussed.

2. Background of PRS and dark-field microscopy

For metal nanoparticles whose diameters (d) are far smaller than the wavelength of the incident light (λ), the abundant surface electrons in metals will oscillate with the external light as shown in Fig. 1A [23,24]. When the oscillation frequency of surface electrons and incident photonics are overlapped, LSPR will occur inducing an enhanced particle-light interaction. LSPR phenomenon of metal nanoparticles leads to strong extinction including absorption and scattering of light [25]. The extinction property of gold nanoparticles (GNPs) has been discovered and applied 1600 years ago. The "Lycurgus Cup" from ancient Rome containing GNPs can change the color at different light irradiation directions: red color with light from the rear (absorption) and green color with light from the front (scattering) as illustrated in Fig. 1B. Following the rapidly developed modern science, the LSPR effect has been widely applied in the fields of pharmacy, life science, and electrocatalysis [26].

From 2000, the advent of dark-field microscopy (DFM) enabled the observation of the scattering light of a single plasmonic nanoparticle, which dramatically promoted the application of LSPR from tubes to nanoscale dimension, even down to single molecular level [27,28]. The PRS light is a kind of Rayleigh scattering without energy loss, thus the scattering wavelength is the same as the incident light, which cannot be separated by the optical filter. DFM employs side illumination method that the incident light irradiates on the samples with an angle after passing through a dark-field condenser (Fig. 1C) [23]. With a transparent substrate, the excitation light will transfer along with the incident direction. The generated isotropous PRS light could be collected by the objective lens and captured by a color camera to give dark-field images (colorful stars) or through a spectrometer and highly sensitive charge-coupled device (CCD) to give scattering spectra (Fig. 1C). Particularly, the PRS cross section σ_{sca} is sensitive to the size, shape, composition, and environmental refractive index of the particles as depicted in Eq. (1−3) [1,6,29]. Particles with larger size and shape factor will lead to spectral redshifts. For instance, gold nanospheres usually show green scattering light at a spectral range of 540 to 580 nm; while gold nanorods always exhibit a red color located from 600 to 800 nm [12,30]. On the other hand, the plasmon resonance bands of silver and gold nanospheres exhibit blue and green colors, respectively [31]. Therefore, color-coded single nanoparticle probes have been constructed by tuning the PRS bands with ultra-high sensitivity and spatial resolution [32]. Moreover, this visualized colorimetric detection is measured only by the DFM cameras without the expensive spectrometer and CCD setup, which is time-saver and low-cost.

$$\sigma_{sca} = \frac{8\pi^3}{3\lambda^4}\alpha^2 \tag{1}$$

$$\alpha = 3V\frac{\varepsilon - \varepsilon_m}{\varepsilon + 2\varepsilon_m} \tag{2}$$

$$\alpha \approx \frac{V}{\left(L + \frac{\varepsilon_m}{\varepsilon - \varepsilon_m}\right) + A\varepsilon_m\chi^2 + B\varepsilon_m^2\chi^4 - i\frac{4\pi^2\varepsilon_m^{3/2}}{3}\frac{V}{\lambda^3}} \tag{3}$$

Eq. (2) represents the ideal nanospheres, while Eq. (3) represents prolate spheroids. Here, α

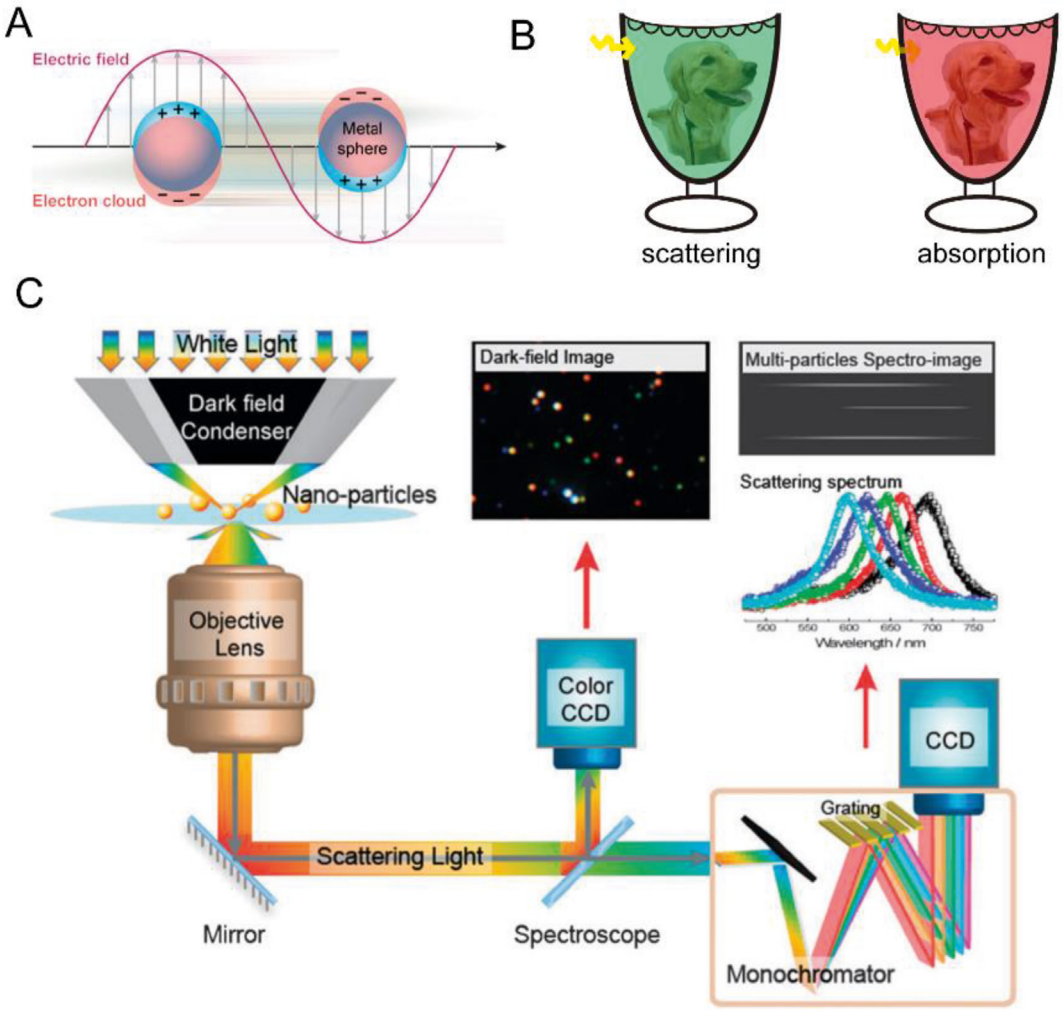

Fig. 1. (A) Interaction between incident electric field and surface electron cloud of metal nanoparticles. (B) Scheme of the "Lycurgus Cup" excited from different directions. (C) Typical dark-field microscopy and spectroscopy setup. Reproduced with permission from Ref. [23], copyright 2012 Royal Society of Chemistry.

is the polarizability, V is the volume of the particle, ε is the dielectric constant of the particle, ε_m is the dielectric constant of the surroundings, L is the shape factor, and χ is the size parameter, A and B are functions of L in longitude and transverse directions, respectively.

3. Color-coded sensors

3.1. Size and composition dependent sensors

The specific plasmon resonance scattering colors enable the characterization of the morphology and composition changes of a single nanoparticle, which is critical for the precise fabrication of nanomaterials. For instance, the electrodeposition and dissolution processes of single Ag, Au and Cu nanoparticles were monitored by PRS color changes, that the scattering light always red shifts during the enlargement of nanoparticles [33–38]. As shown in Fig. 2, a SP1 nanopore array was used as the template, thus, the electron could only be transferred through the nanopore while the nearby membrane is non-conductive. This work offers an approach for the monitoring of the nano-confined reactions in a single nanopore. Moreover, the aging of copper nanoparticles was recognized by the scattering color fading [39]. The freshly electrodeposited Cu nanoparticles showed a noticeable redshift from green to red as the size increased. When the potential was off, the red color slowly dimed due to the oxidation of Cu nanoparticles to CuO_x. On the other hand, the formation of core-shell nanostructures will cause more interesting PRS changes resulting from both the morphology and composition alternations. A 5 nm Ag film deposited on gold nanostars induced that the PRS spectra red shifted ca. 100 nm and the scattering light changed from near-infrared range to visible red color [40]. Utilizing the featured plasmon

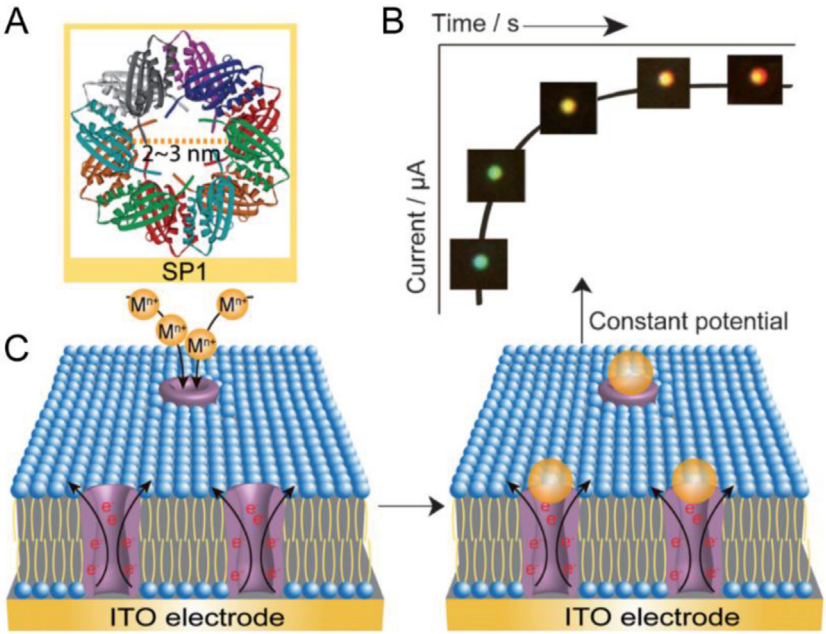

Fig. 2. Electrodeposition in the SP1 generated nanochannels, and Ag, Au, and Cu NPs deposited on the SP1-HBM/ITO template using a developing solution of $AgClO_4$, $HAuCl_4$, and $CuSO_4$ with the standard deposition potentials of 0.05, 0.05, and 0.6 V vs. Ag/AgCl, respectively. (A) Structure of SP1. (B) The images of typical color changes of a single Ag NP changing from blue to red, as the electrodeposition time is increased, indicating the in-situ and real-time monitoring of the growth process of single NPs. (C) SP1-HBM/ITO template. Reproduced with permission from Ref. [34], copyright 2012 Wiley.

resonance of Au and Ag nanoparticles, PRS-tunable Au-Ag alloyed nanoislands were fabricated. The nanoalloy consisted of color filter mosaic could be easily controlled in the visible range through different Au-Ag ratios, which is a promising imaging material in the future displays [41].

Except metals, the surface decoration by non-metal elements and materials were investigated to expand the applications of plasmonic particles. The *in-situ* growth of electrodeposited single Au@Hg nanoalloys was monitored by the visual color changes and spectral shifts [42,43]. During the adsorption and diffusion of Hg atoms into Au nanoparticles, the PRS spectra of Au@Hg nanoalloys exhibited a blueshift with a subsequent red shift. The real-time scattering light changes indicated the interaction between Au and Hg during the Au amalgamation process and the nanoalloys could be on-site controlled by modulating the growth time and applied potentials. Metal@-semiconductor core-shell structures were developed through electrochemical depositions of ZnS, CdSe and CdS on the gold nanoparticle surface [44]. The spectral redshift and color changes showed the dynamic deposition process, and realized the tailor of geometry and resonance bands of nanoalloys, which could be functioned as specific photocatalysts.

Benefitting from the PRS sensitivity to the nanostructures, a series of visual nanosensors have been constructed with ultra-high sensitivity and selectivity. Utilizing the catalytic ability of GNPs, an elegant adenosine triphosphate (ATP) sensor was developed [45]. In the presences of $HAuCl_4$ and glucose, small gold nanoparticles will grow into larger particles, leading to the change of PRS color from green to red. However, when the GNPs were modified with aptamer, the catalytic property of GNPs would be inhibited. With the treatment of ATP, the aptamer was removed from the gold surface and re-activated the GNPs growth to red color. This method achieved the detection of ATP as low as $nmol \cdot L^{-1}$ with high selectivity. Similarly, the etching process of plasmonic nanoprobes have been applied in the detection of pyrophosphate, permanganate and pesticides according to the PRS color changes [46−48]. The metabolism of HeLa cells has been monitored *in vitro* according to the reduced nicotinamide adenine dinucleotide (NADH) mediated deposition of Cu on the GNPs surface to form a core-shell structure as shown in Fig. 3 [49]. The incubated GNPs in HeLa cells exhibited green color which is changed into red/orange color after the addition of copper ions, indicating the presence of cellular NADH. Furthermore, this method has been applied in the screening of anticancer drugs of taxol which could affect the cellular metabolism by inhibiting the generation of NADH. This NADH mediated reduction of copper ions has also been applied in

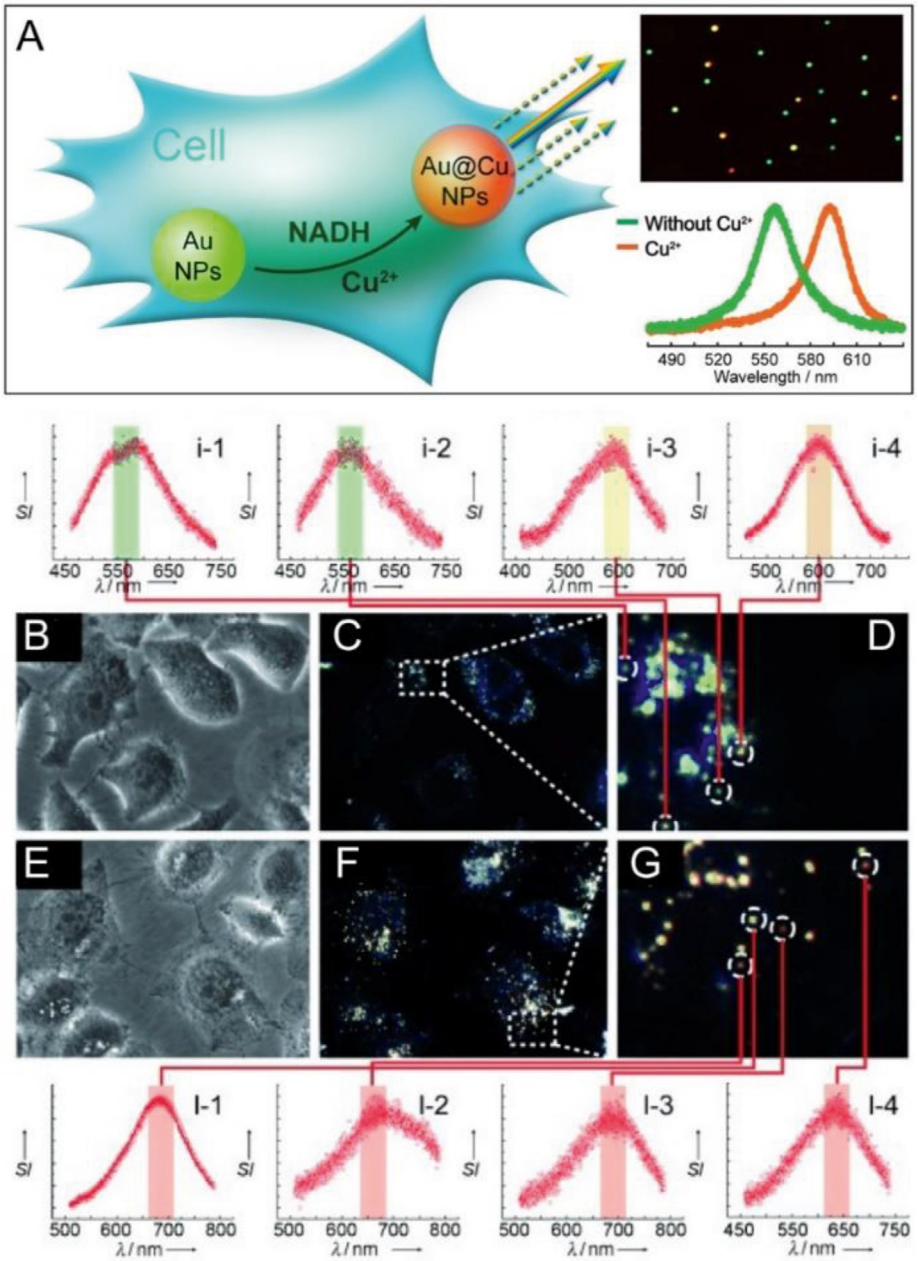

Fig. 3. (A) Scheme showing the growth of GNP seeds by the NADH-catalyzed deposition of a Cu shell in a living cell. (B) Bright-field image of HeLa cells containing GNPs with treatment by taxol (10 mmol·L^{-1}) and then incubation in 50 mmol·L^{-1} $CuCl_2$ for 3 h. (C) DFM image of corresponding HeLa cell in (B). (D) The detail view of HeLa cell DFM images; i-1 to i-4: corresponding scattering spectra of different GNPs in living HeLa cell. (E) Bright-field image of HeLa cells containing GNPs without treatment by taxol and then incubation in 50 mmol·L^{-1} $CuCl_2$ for 3 h. (F) DFM image of corresponding HeLa cell in (E). (G) The detail view of HeLa cell DFM images; I-1to I-4: corresponding scattering spectra of different Au@Cu core-shell NPs in living HeLa cells. Reproduced with permission from Ref. [49], copyright 2011 Wiley.

the colorimetric quantitative detection of pyrophosphate [50].

3.2. Inter-particle coupling based sensors

When two or more plasmonic nanoparticles get close (less than 5 nm), inter-particle coupling will occur inducing distinct PRS spectra redshift and intensity increase [51]. Ultra-sensitive sensors, even single molecule detection can be probed by combining nanoparticles via various linkers [52]. A molecular ruler was constructed by single-stranded DNA linked Au-Au and Ag-Ag dimers [53]. Upon the DNA hybridization process, the PRS spectra of particle pairs showed a blueshift that the rough double-stranded DNA increased the inter-particle distance and weakened the plasmon coupling. Furthermore, hybridized and unpaired DNA chains could be clearly recognized according to the color changes of plasmonic nanoparticles [54]. In

addition, the carbohydrate-protein interaction was detected by coupling two GNPs with protein concanavalin A and dextran [55]. In addition to the biomolecule interactions, a copper ions sensor was constructed by inter-particle coupling arising from the Cu^{+}-catalyzed click reaction as shown in Fig. 4 [56]. Alkyne- and azide-functionalized GNPs would be cross linked in the presences of Cu^{2+} and sodium ascorbate, leading to the color change of GNPs from green to red with obvious spectral redshift. The click reaction linked GNPs enables the detection of copper ions down to nmol·L^{-1} with high selectivity. Moreover, the strong coupling between nanoparticles and plasmon substrates was investigated by an *in-situ* polymerization process in between the particles and substrate [57]. This controllable plasmon coupling offers an excellent colorimetric sensing platform for applications in different fields.

3.3. Converted color-coded single particle detection

The DFM based colorimetric detection enables the visualization of individual particles at nanoscale dimensions, with high sensitivity and low lost, without the spectrometer and gratings setup. Nevertheless, the recognition of the colors of plasmonics is mainly based on the naked eyes and it is difficult to distinguish the subtle color changes (less than 20 nm wavelength shift), which limits its applications. To overcome this problem, many methods have been conceived to enhance the color recognition ability.

The color of PRS light was transformed into corresponding readable tricolor system RGB values to enhance the color resolution [32]. The percentage of each RGB channel intensity was applied to characterize the PRS spectral shift. By this means, the interaction between GNPs and small organic molecules was observed. In the presence of H_2S, Ag particles will be oxidized into AgS resulting in the distinct PRS change [58]. Using the R/G intensity ratio, a facile H_2S sensor was proposed with single Au@Ag probes. In addition, the galvanic exchange process of Ag NPs and Au^{3+} was real-time monitored through a digital RGB three-channel method [59]. Based on a pixel by pixel statistical analysis of the RGB information, plasmonic nanoparticles were employed in the observation of epidermal growth factor receptors (EGFR) in living cells [60]. To further enhance the PRS signal extraction in the living cells, a bias-modified fuzzy C-means algorithm was applied to reduce the strong scattering background of cell itself [61]. Moreover, the conversion from PRS color into HSI (hue (H),saturation (S) and intensity (I)) color system was exploited in the color-coded single particle sensing to precisely distinguish the color changes [62,63]. Assisted by artificial intelligence, the false positive results and background signal will be eliminated to intensively improve the color recognition efficiency and precision [64].

The collection of PRS spectra is generally recorded by a spectrometer and a highly sensitive CCD, which is time consumed and high cost. A facile chrominance-coded method was developed to estimate the PRS spectra peak position and corresponding diameter of single GNPs as shown in Fig. 5A [65]. The captured dark-field image of GNPs was converted into RGB values and then transformed into spectral wavelength based on the chromaticity diagram. Subsequently, the obtained spectral peak wavelength was used to calculate the diameter of the nanospheres according to the Mie theory. Benefitting to a rapid signal recognition program, this method enables the high-throughput measurement of thousands of nanoparticles in the dark-field images (Fig. 5B–D).

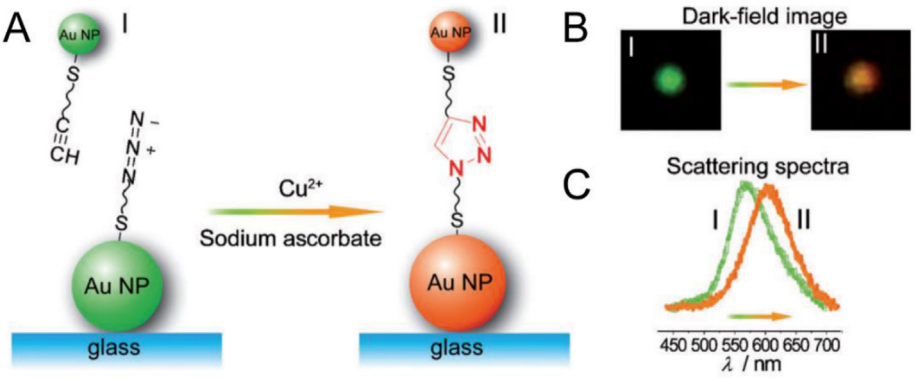

Fig. 4. (A) Cu^{+}-catalyzed click reaction at the single-particle level. (B) A typical dark-field image of a modified GNP on a microscopic slide before (I) and after (II) the additions of Cu^{2+} and sodium ascorbate. (C) Corresponding scattering spectra of a single GNP before (I) and after (II) the click reaction. Reproduced with permission from Ref. [56], copyright 2013 Wiley.

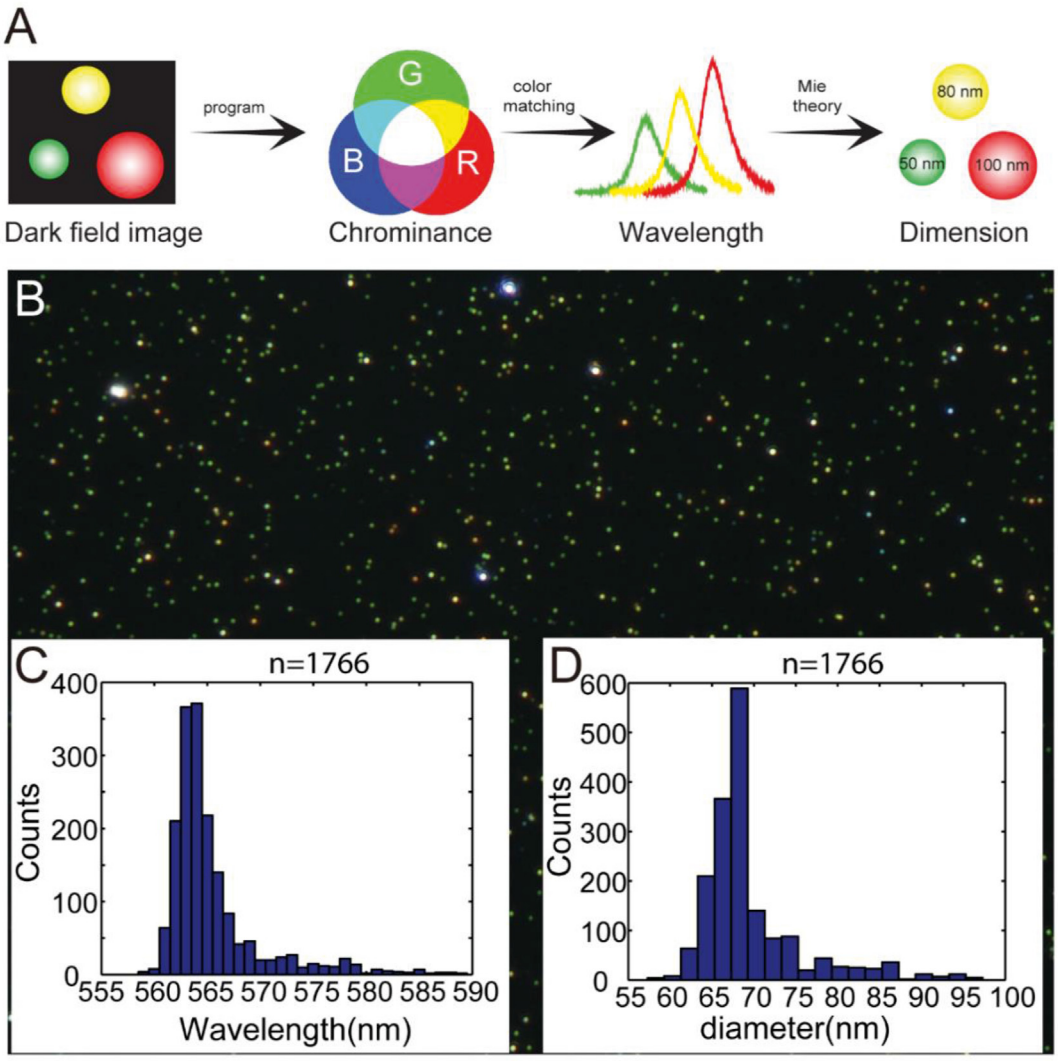

Fig. 5. (A) Scheme of the conversion from PRS light color to RGB values, spectral wavelength and corresponding particle diameter. (B) Dark-field image of mono-dispersed gold nanospheres. (C) Calculated spectral wavelength of the 1766 nanoparticles in the dark-field image in (B). (D) Calculated diameters of the 1766 nanoparticles. Reproduced with permission from Ref. [65], copyright 2012 American Chemical Society.

Utilizing a digital CMOS camera, the time resolution of the colorimetric approach could further be improved which has been applied in biosensors and particle recognition [64,66].

3.4. Polarized scattering light

For the anisotropic nanoparticles such as nanorods, the plasmon resonance modes at different directions could be revealed with polarized incident light. For instance, for a single nanorod with longitudinal and transverse resonance modes, rainbow colors from green, yellow to red were revealed at different polarization angles [67]. A gold nanorod based core-satellite nanoprobe was constructed as a microRNA-21 biosensor under polarized irradiation [68]. The transverse PRS light of gold nanorod is green color, which will shift to red color upon the coupling with the satellite particles linked by microRNA-21 molecules. Moreover, color-selective plasmonic nanoarrays were fabricated to fine control the PRS features with different nanostructures and periodicities [69]. Based on the polarization-dependent PRS light, an aluminum disk array was fabricated so that the PRS color could be modulated by the disk size and gap distance from blue to cyan. When the x- and y-periods are asymmetric, it will exhibit different colors under x-/y-polarized incident light. A four-level security print was thus constructed by encoding the information in the x- and y-periodicities [70].

3.5. From true color to fake color

Combining DFM with electrochemistry is capable of *in-situ* electrochemical detection at nanoscale. For instance, the electrooxidation of glucose, the intermolecular electron transfer and charging process have been investigated by the

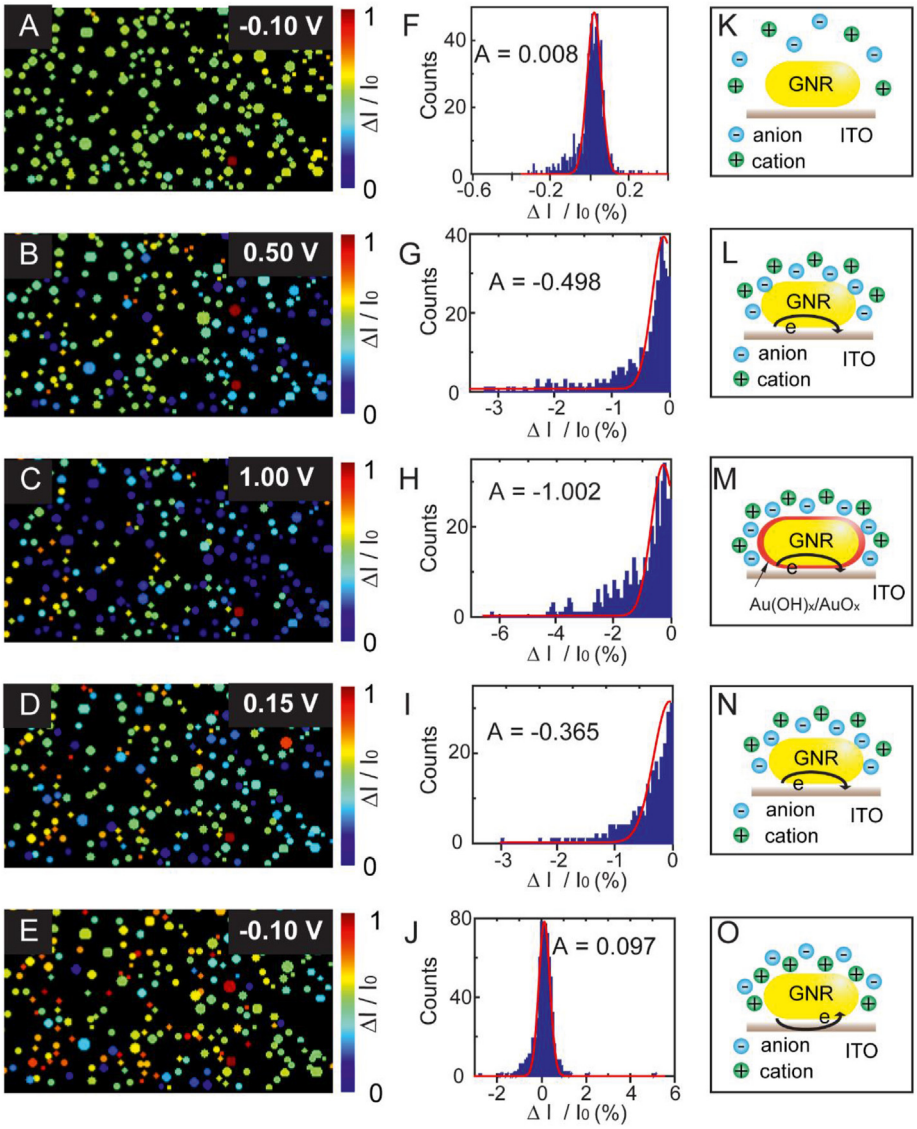

Fig. 6. (A—E) Calculated intensity change ($\Delta I/I_0$) of different nanoparticles in a dark-field image during CV scanning from −0.10 V to 1.00 V and then to −0.10 V in 0.1 mol·L^{-1} KNO_3 solution, at a scan rate of 10 mV·s^{-1} vs. a Pt quasi-reference electrode. (F—J) Statistical intensity change distributions and averaged results of every single nanoparticle in the dark-field image during CV scanning corresponding to the potential in (A—E). Results with the increased intensity in (G—I) were not taken into consideration. (K—O) Proposed redox reaction process of gold nanoparticles during CV scanning corresponding to the potential in (A—E), anions and cations are from the electrolyte. Reproduced with permission from Ref. [74], copyright 2016 Royal Society of Chemistry.

PRS signals [71—73]. However, most of the above mentioned plasmonic sensors are dependent on the true color of the PRS light of the nanoparticles, which is related to the spectral wavelength positions. It is worthy to note that, the scattering intensity also contains abundant sensing information which has rarely used in the visualized measurements. Therefore, a high-throughput method was established to extract and recognize the scattering intensity changes from the dark-field images [74]. To directly visualize the scattering intensity, a signal amplification and conversion program was applied. The PRS signals of particles were firstly transferred into the enhanced intensity values and then were converted into fake colors as shown in Fig. 6. The color distribution represents the intensity alternations. This method was subsequently applied in the *in-situ* monitoring of the electrochemical process. The redox of the plasmonic catalysts and correlated catalytic reactions were clearly distinguished. The high-throughput signal extraction step enables the synchronous observation of thousands of nanoparticles. Both the scattering light intensity distributions of each nanoparticle and the averaged values at each potential could be dynamically captured with a time resolution of ms and a nanoscale spatial resolution. The real-time heterogeneity of each individual

nanoparticle was obviously revealed from the color difference during the electrochemical reactions. Furthermore, by combining this color-code method with plasmon resonance energy transfer, the electrochemical redox of polymerized dyes were *in-situ* investigated with ultra-high sensitivity, even down to single molecule level [75].

4. Conclusions

The unique PRS properties of plasmonic nanoparticles have been discovered and applied for many years. Benefitting from the development of nanotechnology, the deep understanding of the inherent PRS fundamentals has promoted the wide applications of plasmonics in different areas including lift science, environment, and catalysis. This review has summarized the color-coded sensing of single nanoparticles using dark-field microscopy, especially in the field of nano-electrochemistry. The visualized colorful PRS light of nanoparticles was successfully modulated by altering the size, shape and composition, as well as the inter-particle coupling. Thus, facile sensors have been developed with ultra-high sensitivity and time/spatial resolution. It is worthy to note that the development of fine controllable and color-selective nanostructures is still challengeable. Especially, the complex materials with multiple functions such as magnetics, photocatalysts and electrocatalysts are promising probes in the field of sustainable energy resource. Furthermore, high-throughput and multi-channel methods are urgently necessary to enhance the measurement efficiency which is critical for *in-situ* and operando detections.

Acknowledgements

This work was supported by the "Transformational Technologies for Clean Energy and Demonstration," Strategic Priority Research Program of the Chinese Academy of Sciences (Grant No. XDA2100000), National Natural Science Foundation of China (No. 21802042), Shanghai Sailing Program (18YF1405700).

References

[1] Kuwata H, Tamaru H, Esumi K, Miyano K. Resonant light scattering from metal nanoparticles: practical analysis beyond Rayleigh approximation[J]. Appl. Phys. Lett., 2003, 83(22): 4625.

[2] Homola J, Yee S S, Gauglitz G. Surface plasmon resonance sensors: review[J]. Sens. Actuat. B Chem., 1999, 54(1−2): 3−15.

[3] Eustis S, El-Sayed M A. Why gold nanoparticles are more precious than pretty gold: noble metal surface plasmon resonance and its enhancement of the radiative and nonradiative properties of nanocrystals of different shapes [J]. Chem. Soc. Rev., 2006, 35(3): 209−217.

[4] Jing C, Reichert J. Nanoscale electrochemistry in the "dark-field"[J]. Curr. Opin. Electrochem., 2017, 6(1): 10−16.

[5] Hu M, Novo C, Funston A, Wang H, Staleva H, Zou S, Mulvaney P, Xia Y, Hartland G V. Dark-field microscopy studies of single metal nanoparticles: understanding the factors that influence the linewidth of the localized surface plasmon resonance[J]. J. Mater. Chem., 2008, 18(17): 1949−1960.

[6] Anker J N, Hall W P, Lyandres O, Shah N C, Zhao J, Van Duyne R P. Biosensing with plasmonic nanosensors[J]. Nat. Mater., 2008, 7(6): 442−453.

[7] Ma Y, Highsmith A L, Hill C M, Pan S. Dark-Field scattering spectroelectrochemistry analysis of hydrazine oxidation at Au nanoparticle-modified transparent electrodes[J]. J. Phys. Chem. C., 2018, 122(32): 18603−18614.

[8] Wonner K, Evers M V, Tschulik K. Simultaneous opto- and spectro-electrochemistry: reactions of individual nanoparticles uncovered by dark-field microscopy[J]. J. Am. Chem. Soc., 2018, 140(40): 12658−12661.

[9] Wang H H, He T, Du Y, Wang W H, Shen Y B, Li S P, Zhou X C, Yang F. Evolution of single nanobubbles through multi-state dynamics[J]. Chin. Chem. Lett., 2020, 31(9): 2442−2446.

[10] Wang Y X, Shan X N, Tao N J. Emerging tools for studying single entity electrochemistry[J]. Faraday Discuss., 2016, 193: 9−39.

[11] Oja S M, Wood M, Zhang B. Nanoscale electrochemistry[J]. Anal. Chem., 2013, 85(2): 473−486.

[12] Novo C, Funston A M, Gooding A K, Mulvaney P. Electrochemical charging of single gold nanorods[J]. J. Am. Chem. Soc., 2009, 131(41): 14664−14666.

[13] Jing C, Long Y T. Observing electrochemistry on single plasmonic nanoparticles[J]. Electrochem. Sci. Adv., 2021, 2(4): e2100115.

[14] Shang J, Fan J S, Qin W W, Li K. Single-particle measurements of nanocatalysis with dark-field microscopy[J]. Catalysts, 2022, 12(7): 764.

[15] Olson J, Dominguez-Medina S, Hoggard A, Wang L Y, Chang W S, Link S. Optical characterization of single plasmonic nanoparticles[J]. Chem. Soc. Rev., 2015, 44(1): 40−57.

[16] Wang H H, Zhang T, Zhou X C. Dark-Field spectroscopy: development, applications and perspectives in single nanoparticle catalysis[J]. J. Phys.: Condens. Matter, 2019, 31(47): 473001.

[17] Asiala S M, Marr J M, Gervinskas G, Juodkazis S, Schultz Z D. Plasmonic color analysis of Ag-coated black-Si SERS substrate[J]. Phys. Chem. Chem. Phys., 2015, 17(45): 30461−30467.

[18] Rodriguez-Fajardo V, Sanz V, de Miguel I, Berthelot J, Acimovic S S, Porcar-Guezenec R, Quidant R. Two-color dark-field (TCDF) microscopy for metal nanoparticle imaging inside cells[J]. Nanoscale, 2018, 10(8): 4019−4027.

[19] Alberti G, Zanoni C, Magnaghi L R, Biesuz R. Gold and silver nanoparticle-based colorimetric sensors: new trends and applications[J]. Chemosensors, 2021, 9(11): 305.

[20] Wang S M, Wang H, Zhao W, Xu J J, Chen H Y. Single-particle detection of cholesterol based on the host-guest recognition induced plasmon resonance energy transfer[J]. Chin. Chem. Lett. 2022: 108053.

[21] Liu G Y, Lu M, Huang X D, Li T F, Xu D H. Application of gold-nanoparticle colorimetric sensing to rapid food safety screening[J]. Sensors, 2018, 18(12): 4166.

[22] Sharma R, Dhillon A, Kumar D. Mentha-stabilized silver nanoparticles for high-performance colorimetric detection of Al(III) in aqueous systems[J]. Sci. Rep., 2018, 8(1): 5189.

[23] Li Y, Jing C, Zhang L, Long Y T. Resonance scattering particles as biological nanosensors *in vitro* and *in vivo*[J]. Chem. Soc. Rev., 2012, 41(2): 632−642.
[24] Hafner J H, Mayer K M. Localized surface plasmon resonance sensors[J]. Chem. Rev., 2011, 111(6): 3828−3857.
[25] Kelly K L, Coronado E, Zhao L L, Schatz G C. The optical properties of metal nanoparticles: the influence of size, shape, and dielectric environment[J]. J. Phys. Chem. B, 2003, 107(3): 668−677.
[26] Stewart M E, Anderton C R, Thompson L B, Maria J, Gray S K, Rogers J A, Nuzzo R G. Nanostructured plasmonic sensors[J]. Chem. Rev., 2008, 108(2): 494−521.
[27] Sonnichsen C, Geier S, Hecker N E, von Plessen G, Feldmann J, Ditlbacher H, Lamprecht B, Krenn J R, Aussenegg F R, Chan V ZH, Spatz J P, Moller M. Spectroscopy of single metallic nanoparticles using total internal reflection microscopy[J]. Appl. Phys. Lett., 2000, 77(19): 2949−2951.
[28] Schultz D A, Schultz S, Smith D R, Mock J J. Single-target molecule detection with nonbleaching multicolor optical immunolabels[J]. Proc. Natl. Acad. Sci., 2000, 97(3): 996−1001.
[29] Nehl C L, Liao H, Hafner J H. Optical properties of star-shaped gold nanoparticles[J]. Nano Lett., 2006, 6(4): 683−688.
[30] Jain P K, El-Sayed I H, El-Sayed M A. Au nanoparticles target cancer[J]. Nano Today, 2007, 2(1): 18−29.
[31] Mock J J, Barbic M, Smith D R, Schultz D A, Schultz S. Shape effects in plasmon resonance of individual colloidal silver nanoparticles[J]. J. Chem. Phys., 2002, 116(15): 6755−6759.
[32] Liu Y, Ling J, Huang C Z. Individually color-coded plasmonic nanoparticles for rgb analysis[J]. Chem. Commun., 2011, 47(28): 8121−8123.
[33] Hill C M, Pan S. A Dark-Field scattering spectroelectrochemical technique for tracking the electrodeposition of single silver nanoparticles[J]. J. Am. Chem. Soc., 2013, 135(46): 17250−17253.
[34] Qin L X, Li Y, Li D W, Jing C, Chen B Q, Ma W, Heyman A, Shoseyov O, Willner I, Tian H, Long Y T. Electrodeposition of single-metal nanoparticles on stable protein 1 membranes: application of plasmonic sensing by single nanoparticles[J]. Angew. Chem. Int. Ed., 2012, 51(1): 140−144.
[35] Hill C M, Bennett R, Zhou C, Street S, Zheng J, Pan S. Single Ag nanoparticle spectroelectrochemistry via dark-field scattering and fluorescence microscopies[J]. J. Phys. Chem. C., 2015, 119(12): 6760−6768.
[36] Wonner K, Rurainsky C, Tschulik K. Operando studies of the electrochemical dissolution of silver nanoparticles in nitrate solutions observed with hyperspectral dark-field microscopy[J]. Front Chem., 2019, 7: 912.
[37] Sun S S, Gao M X, Lei G, Zou H Y, Ma J, Huang C Z. Visually monitoring the etching process of gold nanoparticles by KI/I_2 at single-nanoparticle level using scattered-light dark-field microscopic imaging[J]. Nano Res., 2016, 9(4): 1125−1134.
[38] Hu S, Yi J, Zhang Y J, Lin K Q, Liu B J, Chen L, Zhan C, Lei Z C, Sun J J, Zong C, Li J F, Ren B. Observing atomic layer electrodeposition on single nanocrystals surface by dark field spectroscopy[J]. Nat. Commun., 2020, 11(1): 2518.
[39] Qin L X, Jing C, Li Y, Li D W, Long Y T. Real-time monitoring of the aging of single plasmonic copper nanoparticles[J]. Chem. Commun., 2012, 48(10): 1511−1513.
[40] Chirea M, Collins S S, Wei X, Mulvaney P. Spectroelectrochemistry of silver deposition on single gold nanocrystals[J]. J. Phys. Chem. Lett., 2014, 5(24): 4331−4335.
[41] Hwang C SH, Ahn M S, Lee Y, Chung T, Jeong K H. Ag/Au alloyed nanoislands for wafer-level plasmonic color filter arrays[J]. Sci. Rep., 2019, 9(1): 9082.
[42] Wang J G, Fossey J S, Li M, Xie T, Long Y T. Real-time plasmonic monitoring of single gold amalgam nanoalloy electrochemical formation and stripping[J]. ACS Appl. Mater. Interface, 2016, 8(12): 8305−8314.
[43] Liu Y, Huang C Z. Real-time dark-field scattering microscopic monitoring of the *in-situ* growth of single Ag@Hg nanoalloys[J]. ACS Nano, 2013, 7(12): 11026−11034.
[44] Wang H, Zhao W, Xu C H, Chen H Y, Xu J J. Electrochemical synthesis of Au@semiconductor core-shell nanocrystals guided by single particle plasmonic imaging[J]. Chem. Sci., 2019, 10(40): 9308−9314.
[45] Liu Q, Jing C, Zheng X, Gu Z, Li D, Li D W, Huang Q, Long Y T, Fan C. Nanoplasmonic detection of adenosine triphosphate by aptamer regulated self-catalytic growth of single gold nanoparticles[J]. Chem. Commun., 2012, 48(77): 9574−9576.
[46] Gu X Y, Liu J J, Gao P F, Li Y F, Huang C Z. Gold triangular nanoplates based single-particle dark-field microscopy assay of pyrophosphate[J]. Anal. Chem., 2019, 91(24): 15798−15803.
[47] Ye Z J, Weng R, Ma Y H, Wang F Y, Liu H, Wei L, Xiao L H. Label-free, single-particle, colorimetric detection of permanganate by GNPs@Ag core-shell nanoparticles with dark-field optical microscopy[J]. Anal. Chem., 2018, 90(21): 13044−13050.
[48] Huang M N, Fan Y P, Yuan X, Wei L. Color-coded detection of malathion based on enzyme inhibition with dark-field optical microscopy[J]. Sens. Actuat. B Chem., 2022, 353(15): 131135.
[49] Zhang L, Li Y, Li D W, Jing C, Chen X, Lv M, Huang Q, Long Y T, Willner I. Single gold nanoparticles as real-time optical probes for the detection of NADH-dependent intracellular metabolic enzymatic pathways[J]. Angew. Chem. Int. Ed., 2011, 50(30): 6789−6792.
[50] Qi F, Han Y M, Ye Z J, Liu H, Wei L, Xiao L H. Color-coded single-particle pyrophosphate assay with dark-field optical microscopy[J]. Anal. Chem., 2018, 90(18): 11146−11153.
[51] Pini V, Kosaka P M, Ruz J J, Malvar O, Encinar M, Tamayo J, Calleja M. Spatially multiplexed dark-field microspectrophotometry for nanoplasmonics[J]. Sci. Rep., 2016, 6: 22836.
[52] Ghosh S K, Pal T. Interparticle coupling effect on the surface plasmon resonance of gold nanoparticles: from theory to applications[J]. Chem. Rev., 2007, 107(11): 4797−4862.
[53] Sonnichsen C, Reinhard B M, Liphardt J, Alivisatos A P. A molecular ruler based on plasmon coupling of single gold and silver nanoparticles[J]. Nat. Biotechnol., 2005, 23(6): 741−745.
[54] Xiao L, Wei L, He Y, Yeung E S. Single molecule biosensing using color coded plasmon resonant metal nanoparticles[J]. Anal. Chem., 2010, 82(14): 6308−6314.
[55] Jin H Y, Li D W, Zhang N, Gu Z, Long Y T. Analyzing carbohydrate-protein interaction based on single plasmonic nanoparticle by conventional Dark Field microscopy [J]. ACS Appl. Mater. Interface, 2015, 7(22): 12249−12253.
[56] Shi L, Jing C, Ma W, Li D W, Halls J E, Marken F, Long Y T. Plasmon resonance scattering spectroscopy at the single-nanoparticle level: real-time monitoring of a click reaction [J]. Angew. Chem. Int. Ed., 2013, 52(23): 6011−6014.
[57] Ding T, Mertens J, Lombardi A, Scherman O A, Baumberg J J. Light-directed tuning of plasmon resonances via plasmon-induced polymerization using hot electrons[J]. ACS Photonics, 2017, 4(6): 1453−1458.
[58] Hao J, Xiong B, Cheng X, He Y, Yeung E S. High-throughput sulfide sensing with colorimetric analysis of single Au-Ag core-shell nanoparticles[J]. Anal. Chem., 2014, 86(10): 4663−4667.
[59] Zhou J, Yang T, He W, Pan Z Y, Huang C Z. A galvanic exchange process visualized on single silver nanoparticles via dark-field microscopy imaging[J]. Nanoscale, 2018, 10(26): 12805−12812.
[60] Aaron J, Travis K, Harrison N, Sokolov K. Dynamic imaging of molecular assemblies in live cells based on nanoparticle plasmon resonance coupling[J]. Nano Lett., 2009, 9(10): 3612−3618.
[61] Gu Z, Jing C, Ying Y L, He P, Long Y T. *In situ* high throughput scattering light analysis of single plasmonic nanoparticles in living cells[J]. Theranostics, 2015, 5(2): 188−195.

[62] Zhou J, Lei G, Zheng L L, Gao P F, Huang C Z. Hsi colour-coded analysis of scattered light of single plasmonic nanoparticles[J]. Nanoscale, 2016, 8(22): 11467−11471.
[63] Zhou J, Gao P F, Zhang H Z, Lei G, Zheng L L, Liu H, Huang C Z. Color resolution improvement of the dark-field microscopy imaging of single light scattering plasmonic nanoprobes for microrna visual detection[J]. Nanoscale, 2017, 9(13): 4593−4600.
[64] Sriram M, Markhali B P, Nicovich P R, Bennett D T, Reece P J, Brynn Hibbert D, Tilley R D, Gaus K, Vivekchand S RC, Gooding J J. A rapid readout for many single plasmonic nanoparticles using dark-field microscopy and digital color analysis[J]. Biosens. Bioelectron., 2018, 117: 530−536.
[65] Jing C, Gu Z, Ying Y L, Li D W, Zhang L, Long Y T. Chrominance to dimension: a real-time method for measuring the size of single gold nanoparticles[J]. Anal. Chem., 2012, 84(10): 4284−4291.
[66] Wagner T, Lipinski H G, Wiemann M. Dark Field nanoparticle tracking analysis for size characterization of plasmonic and non-plasmonic particles[J]. J. Nanopart. Res., 2014, 16(5): 2419.
[67] Huang Y, Kim D H. Dark-Field microscopy studies of polarization-dependent plasmonic resonance of single gold nanorods: rainbow nanoparticles[J]. Nanoscale, 2011, 3(8): 3228−3232.
[68] Liu J J, Yan H H, Zhang Q, Gao P F, Li C M, Liang G L, Huang C Z, Wang J. High-resolution vertical polarization excited dark-field microscopic imaging of anisotropic gold nanorods for the sensitive detection and spatial imaging of intracellular microrna-21[J]. Anal. Chem., 2020, 92(19): 13118−13125.
[69] Fan J R, Wu W G, Chen Z J, Zhu J, Li J. Three-dimensional cavity nanoantennas with resonant-enhanced surface plasmons as dynamic color-tuning reflectors[J]. Nanoscale, 2017, 9(10): 3416−3423.
[70] Ng R JH, Krishnan R V, Wang H, Yang J KW. Darkfield colors from multi-periodic arrays of gap plasmon resonators[J]. Nanophotonics, 2020, 9(2): 533−545.
[71] Wang J G, Fossey J S, Li M, Li D W, Ma W, Ying Y L, Qian R C, Cao C, Long Y T. Real-time plasmonic monitoring of electrocatalysis on single nanorods[J]. J. Electroanal. Chem., 2016, 781: 257−264.
[72] Zhou H, Liu Q, Rawson F J, Ma W, Li D W, Li D, Long Y T. Optical monitoring of faradaic reaction using single plasmon-resonant nanorods functionalized with graphene[J]. Chem. Commun., 2015, 51(15): 3223−3226.
[73] Cao Y, Zhou H, Qian R C, Liu J, Ying Y L, Long Y T. Analysis of the electron transfer properties of carbon quantum dots on gold nanorod surfaces via plasmonic resonance scattering spectroscopy[J]. Chem. Commun., 2017, 53(42): 5729−5732.
[74] Jing C, Gu Z, Long Y T. Imaging electrocatalytic processes on single gold nanorods[J]. Faraday Discuss., 2016, 193: 371−385.
[75] Jing C, Gu Z, Xie T, Long Y T. Color-coded imaging of electrochromic process at single nanoparticle level[J]. Chem. Sci., 2016, 7(8): 5347−5351.

暗场显微镜下的彩色"纳米星"

静　超[a]，龙亿涛[b,c,*]
[a]中国科学院上海应用物理研究所，上海 201800
[b]生命分析化学国家重点实验室，南京大学化学化工学院，江苏 南京 210023
[c]分子传感与成像中心，南京大学，江苏 南京 210023

摘要

具有独特局域表面等离子共振散射特性的贵金属纳米粒子，在可见光区域表现出明显的吸收和散射光谱特性。在过去的几十年中，基于纳米金和纳米银溶液的可视化颜色传感器，被广泛应用在金属离子、生物分子、农药等灵敏检测。自 2000 年，暗场显微镜的出现，实现了纳米尺度下等离子共振散射光谱的精准获取，将传感尺度从传统的实验试管发展到单纳米颗粒界面。单颗粒检测消除了本体溶液中大量纳米粒子产生的平均效应，可提供更加准确的反应信息。纳米粒子的散射光谱主要取决于颗粒的尺寸、形貌、成分以及颗粒间耦合作用等，因此，具有特定散射颜色的单个纳米粒子，可以作为优异的纳米探针。这篇综述聚焦于单颗粒纳米传感，首先介绍了纳米粒子局域表面等离子共振的原理和发展历史。随后，主要讨论了单个贵金属纳米粒子作为颜色编码传感器，在生物分子、环境污染物以及能源等领域的应用，尤其是基于单颗粒的原位纳米光谱电化学传感及其在电催化反应中的应用。例如，利用纳米粒子的溶出和生长过程，精巧地设计了针对不同待测物的纳米探针。另一方面，对单纳米粒子结构演变过程的原位监测，也有助于对纳米材料制备机理的理解。最后，着重探讨了纳米颜色传感器信号提取放大的检测手段，包括将肉眼识别的颜色转换为可读的三原色信息以及偏振光检测技术等，进一步扩展单颗粒颜色传感的应用范围。

关键词：等离子共振散射；暗场显微镜；颜色传感器；纳米电化学；单颗粒检测